



Synthesizing MePCM from industrial waste-derived nanoparticles via surfactant-free pickering emulsion for building applications under hot climate

Abdin Bedada Huluka^a, S. Muthulingam^{a,*}, S. Manigandan^b, Chandra Shekhar^c

^a Department of Civil Engineering, Indian Institute of Technology Ropar, Rupnagar, 140 001, India

^b Centre of Research for Energy Efficiency and Decarbonization (CREED), Indian Institute of Technology Ropar, Rupnagar 140 001, India

^c Department of Biosystems and Soft Matter, Institute of Fundamental Technological Research Polish Academy of Sciences, Poland

ARTICLE INFO

Keywords:

Expanded polystyrene

Nanoparticles

Pickering emulsion

Microencapsulated phase change material

Building application

ABSTRACT

This study synthesizes microencapsulated phase change materials (MePCM) from industrial waste-derived expanded polystyrene (EPS) nanoparticles using a surfactant-free Pickering emulsion for building applications in hot climates. EPS nanoparticles, synthesized via optimized nanoprecipitation technique with 70 % sonicator amplitude, serve as the MePCM shell with n-eicosane as the core. Characterizations show EPS nanoparticles with diameter of 150 nm and MePCM sizes predominantly around 12 μ m. MePCMs exhibit melting and solidification enthalpies of 301.4 J/g and 298.5 J/g, respectively, highlighting their potential for integration into building materials for enhancing thermal management of buildings in hot climate.

1. Introduction

Phase change materials (PCMs) store and release thermal energy through latent heat during solid-liquid transitions. Organic PCMs, favored for their thermal stability, high latent heat, and minimal supercooling, are widely used in building insulation, solar heating, and electronics [1]. Suitable for space heating and cooling within a 0–65 °C range, their broader use is sometimes limited by leakage and chemical reactions during phase transitions [2]. Encapsulating PCMs within a microscale shell, called microencapsulated PCM (MePCM), prevents leakage, enhances heat transfer by increasing the surface-to-volume ratio, and provides a larger heat exchange surface. This method uses shell materials with higher melting points to encase the melted PCM, preventing leakage [3].

An ideal MePCM shell, specifically for building applications, would: demonstrate strong mechanical and thermal characteristics to prevent breakage; offer high thermal conductivity for effective heat transfer; be chemically inert to avoid change in PCM properties, and be leak-proof to preserve the integrity of surrounding materials [4]. Moreover, shells are commonly made from organic polymers, which offer excellent chemical stability. Inorganic materials like silica and calcium carbonates are also used for their high thermal conductivity [5]. Further, various techniques are used for synthesizing MePCMs, including physico-mechanical methods (e.g. spray drying), chemical methods (e.g. emulsion, polymerization), and physico-chemical methods (e.g. sol-gel) [6].

The literature reveals that MePCMs integrated into construction materials typically involve organic materials (e.g. melamine formaldehyde resin) and inorganic materials (e.g. silica) [6]. To promote environmental sustainability, developing MePCM shells using industrial waste to enable material recycling, reduce pollution, lower raw material costs, and minimize the environmental footprint, advancing sustainable material synthesis is desirable. Traditional MePCM synthesis often uses large quantities of environmentally harmful amphiphilic surfactants. In contrast, surfactant-free Pickering emulsions, which are more stable, are preferable [7]. Note that surfactant-free methods can reduce environmental impact, lower production costs, and achieve smoother microcapsules with enhanced encapsulation efficiency and thermal stability. In this context, the current study synthesizes nanoparticles from expanded polystyrene (EPS) waste for use as shell material in developing MePCMs through a surfactant-free Pickering emulsion process, followed by thermophysical characterization. The synthesis process promotes sustainable development and yields a MePCM suitable for integrating into construction materials to enhance building thermal management, particularly in hot climates.

2. Materials and methods

2.1. Synthesis of shell nanoparticles from waste material

EPS nanoparticles were synthesized using waste materials. Acetone, procured from Sigma-Aldrich, India, was used as a solvent. The

* Corresponding author.

E-mail address: muthulingam.subramaniyan@iitrpr.ac.in (S. Muthulingam).

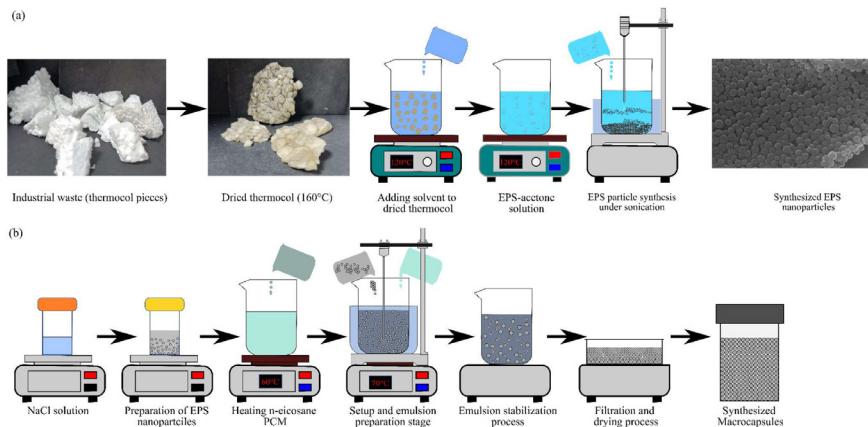


Fig. 1. Schematic of synthesis procedure: (a) EPS nanoparticles; and (b) MePCM.

hydrodynamic radius of the EPS nanoparticles was measured using dynamic light scattering with a Zetasizer Nano ZSP from Malvern Instruments. A probe-type sonicator (Model: Branson SFX 250, output: 250 W) was used at varying amplitudes for 2 min to optimize the nanoparticle size. EPS sourced from leftover packaging materials, was used alongside analytical-grade acetone as a solvent to initiate precipitation. This process resulted in the synthesis of uniform nanoparticles. EPS nanoparticles were synthesized following the nanoprecipitation method outlined in [8], with sonication introduced to achieve better-sized nanoparticles. Fig. 1a illustrates the step-by-step schematic of the EPS synthesis process. Thermocol commonly used in packaging was cut into small pieces and heated at 160 °C for 12hr in a hot air oven to remove volatile substances, causing it to shrink. After removing volatile matter, the thermocol samples were dissolved in acetone at a 1 (EPS):20 (acetone) ratio and magnetic stirred at 500 rpm for 6 h. Impurities were allowed to settle, and the clear solution was transferred to a container. To synthesize nanoparticles, 1 mL of this EPS-acetone solution was gradually added to 20 mL of deionized water at a 0.5mL/min rate under a probe-type sonicator. In this step, the sonicator amplitude is 70 % to deagglomerate nanoparticle clusters and to obtain better-sized nanoparticles. The mixture was then maintained at 25 °C for 8hr and heated to 60 °C for 4 h to evaporate the acetone and any excess solvent, ensuring uniform nanoparticle distribution. Then, the particles were characterized using various techniques.

2.2. Synthesis of MePCM

n-Eicosane, sourced from Sigma-Aldrich Japan, Tokyo, was utilized as the PCM. NaCl, obtained from Sigma-Aldrich, India, was employed as the electrolyte. The synthesis of MePCM was carried out using a Homogenizer (IKA T25 Digital Ultra-Turrax model). n-Eicosane, an organic PCM, having a melting temperature of 36–38 °C is used. This is one of the PCMs used for thermal management of building envelope under hot climate [9]. Fig. 1b illustrates the step-by-step schematic of the MePCM synthesis process using a surfactant-free Pickering emulsion template. Initially, a salt solution is prepared with a 1:1 ratio of NaCl to distilled water, mixed for 3 min using a vortex mixer. EPS nanoparticles are then added to this solution in equal weight and mixed for another 3min. Concurrently, n-eicosane is heated to 60 °C to liquefy. A water bath is also prepared on a hot plate, maintained at 70 °C. The solution is then emulsified using a homogenizer at 10000 rpm for 5min. After homogenization, the emulsion is cooled for 10 min and left to stabilize for 24hr at 25 °C in an incubator. Finally, the microcapsules are isolated using nano filter paper and air-dried at room temperature before further characterization. It is worth pointing out here that, following the established synthesis protocol for MePCM, the core-to-shell ratio is maintained at 10:1. Under the assumption of perfect encapsulation with no losses or imperfections during the synthesis process, the theoretical core material content is cal-

culated to be 90.91 %, with a corresponding theoretical latent heat of 298.18 J/g.

3. Results and discussion

3.1. Microstructural investigation

Fig. 2a depicts the effects of sonicator amplitude and size of EPS nanoparticles. Ultrasonic treatment breaks down large nanoparticle clusters into smaller clusters or individual nanoparticles. As observed, nanoparticle size increases from 10 % to 40 % (a 35 % increase) and subsequently decreases, reaching the lowest at 70 %. Note that smaller nanoparticles have relatively larger surface area and thus potentially can have enhanced thermal conductivity and specific heat capacity, which are favorable for building applications. Smaller particle sizes increase the surface-to-volume ratio, providing more efficient heat transfer pathways and enhancing thermal conductivity [10]. The higher surface area also exposes more surface atoms, which exhibit distinct vibrational properties (surface phonon modes) that elevate the specific heat capacity, as more energy is needed to heat the system. Conversely, larger particles exhibit properties closer to bulk materials, leading to a specific heat capacity that aligns more with bulk material's values, minimizing surface effects [11].

Further, from Fig. 2a, the intensity variation to synthesize nanoparticle size is significant between 0 and 25 %. Thus, a sonicator amplitude of 70 % is suggested to obtain majority nanoparticles. Note that the synthesis of EPS nanoparticles using the solvent method is a nucleation and precipitation process in which soluble polystyrene nucleates from the solution, forming particles in water. 70 % sonication amplitudes were employed during particle synthesis, as illustrated in Fig. 2a. Each 20 mL batch underwent sonication for 2 min at room temperature (25 °C). To minimize temperature fluctuations that could potentially influence particle properties, a water jacket was incorporated around the synthesis reactor. Elevated temperatures during the synthesis process can enhance particle diffusion, leading to changes in particle shape and size. From the analysis at lower amplitude settings (10 %–40 %), particle size increases due to insufficient mixing, leading to particle aggregation/clustering. In contrast, mixing improves significantly at higher amplitudes (50 %–70 %). During sonication, formed bubbles collapse rapidly, generating substantial thrust that enhances mixing within the solution. This results in smaller particle sizes, as rapid mixing facilitates efficient distribution of the organic phase into the aqueous phase, allowing better distribution of polymer chains. Consequently, this leads to a larger number of smaller nuclei, resulting in smaller nanoparticles overall [8], as reflected by Fig. 2a. Note that all datasets presented in this figure were repeated three times to minimize experimental errors.

The characterization of MePCM was performed using FE-SEM, Model No: JSM7610F Plus, along with a DII-29030SCTR smart coater.

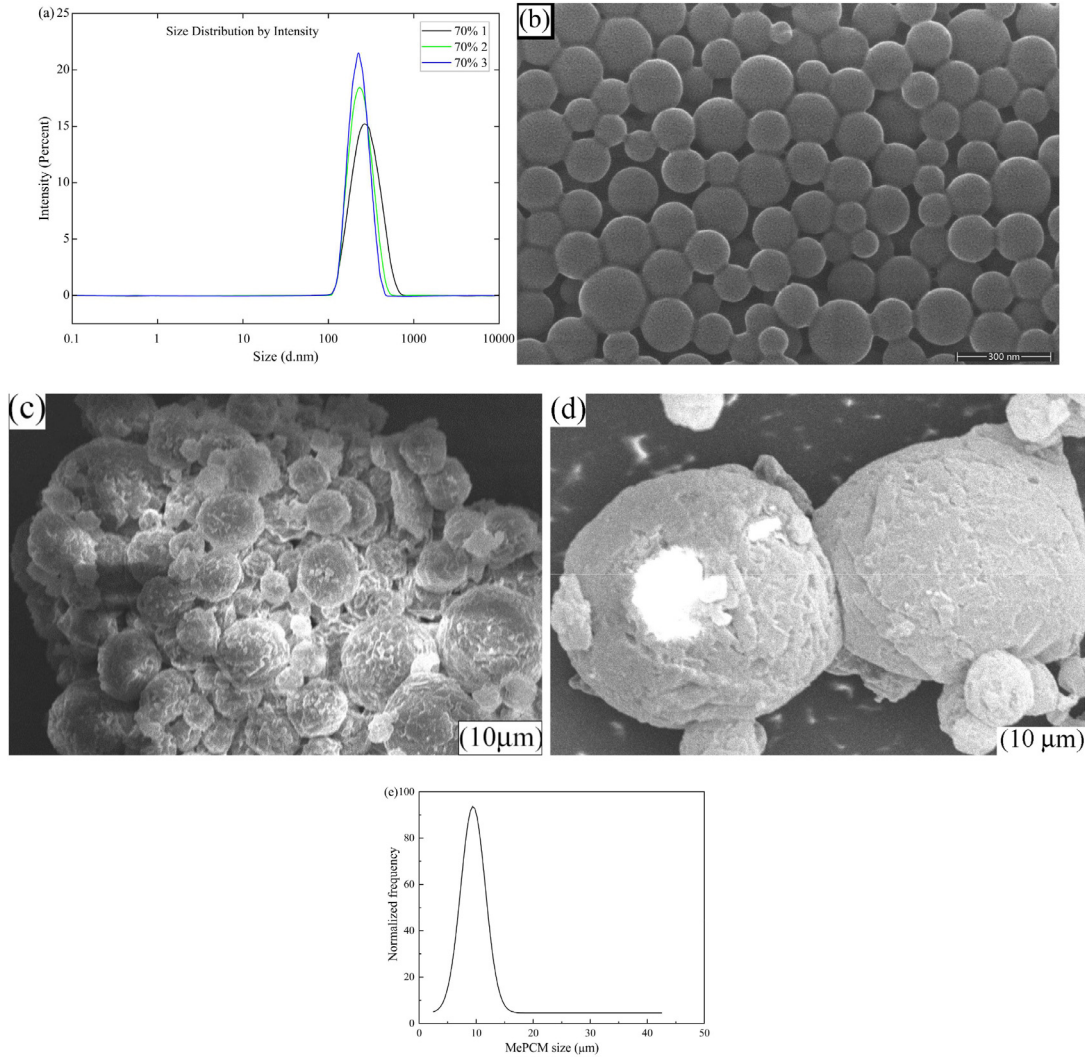


Fig. 2. Microstructural investigation: (a) Sonicator amplitude effect; (b) FE-SEM image of EPS nanoparticles; (c,d) SEM image of MePCM; (e) Size distribution of MePCM.

Fig. 2b shows the synthesized EPS nanoparticles' representative FE-SEM image. The particles produced are predominantly spherical and exhibit slight polydispersity. Many nanoparticles are observed with diameter of 150 nm. Further, Fig. 2c shows a representative SEM image of MePCM. As observed, MePCM shows spherical shapes with n-eicosane concentrated within the EPS nanoparticles shell due to the Pickering effect. On careful examination (Ref. Fig. 2d), it can be observed that the dispersed phase containing n-eicosane spherical emulsions are entirely encapsulated by EPS nanoparticles shell in the first layer, indicating core-shell structural arrangement. Moreover, electron microscopic images showed a smooth inner surface and a rough, undulating outer surface of the microcapsules. Analysis of over 400 MePCMs revealed an average diameter of 12 μm, as shown in Fig. 2e. The size distribution ranged from 3.4 μm to 39.6 μm, with a large number clustering around 12 μm. Given these dimensions align with the voids in building materials, integration for thermal management is highly viable.

3.2. Thermophysical characterization

The heat flow analysis of MePCM was conducted using a NETZSCH DSC 204F1 differential scanning calorimeter (DSC). Fig. 3a presents the DSC thermograms of n-eicosane and MePCM, both showing a single melting peak at 40.9 °C for n-eicosane and 41.8 °C for MePCM. During solidification, both display double peaks with maximum temperatures

of 31.6 °C for n-eicosane and 29.8 °C for MePCM. The double peaks during n-eicosane's exothermic phase indicate a complex solidification involving two phase transitions: from isotropic liquid to rotator phase, and from rotator to crystalline phase. Additionally, Fig. 3a includes the melting and solidification enthalpies for both materials, with MePCM's values at 301.4 J/g and 298.5 J/g, respectively, lower than n-eicosane's 323.5 J/g and 332.5 J/g. Note that the equivalency of melting and solidification enthalpies of MePCM can be attributed to several factors related to the encapsulation process, the materials used for encapsulation, and the structural modifications that occur during microencapsulation. Additionally, the enthalpies of MePCM may be attributed to encapsulation ratio and encapsulation efficiency, which can be calculated as [12]:

$$R = \frac{\Delta H_{m, \text{MePCM}}}{\Delta H_{m, \text{PCM}}} \times 100\% \quad (1)$$

$$E = \frac{\Delta H_{m, \text{MePCM}} + \Delta H_{c, \text{MePCM}}}{\Delta H_{m, \text{MePCM}} + \Delta H_{c, \text{MePCM}}} \times 100\% \quad (2)$$

where R represents encapsulation ratio and E signifies encapsulation efficiency. Table 1 presents the thermal properties of n-eicosane and MePCM. As observed, the encapsulation ratio of MePCM is 93.04 % obtained and the encapsulation efficiency is determined 91.45 % enthalpies.

Moreover, the latent heat enthalpy may be attributed to the energy required for melting and solidifying ion pairs, multiples, clusters, and ag-

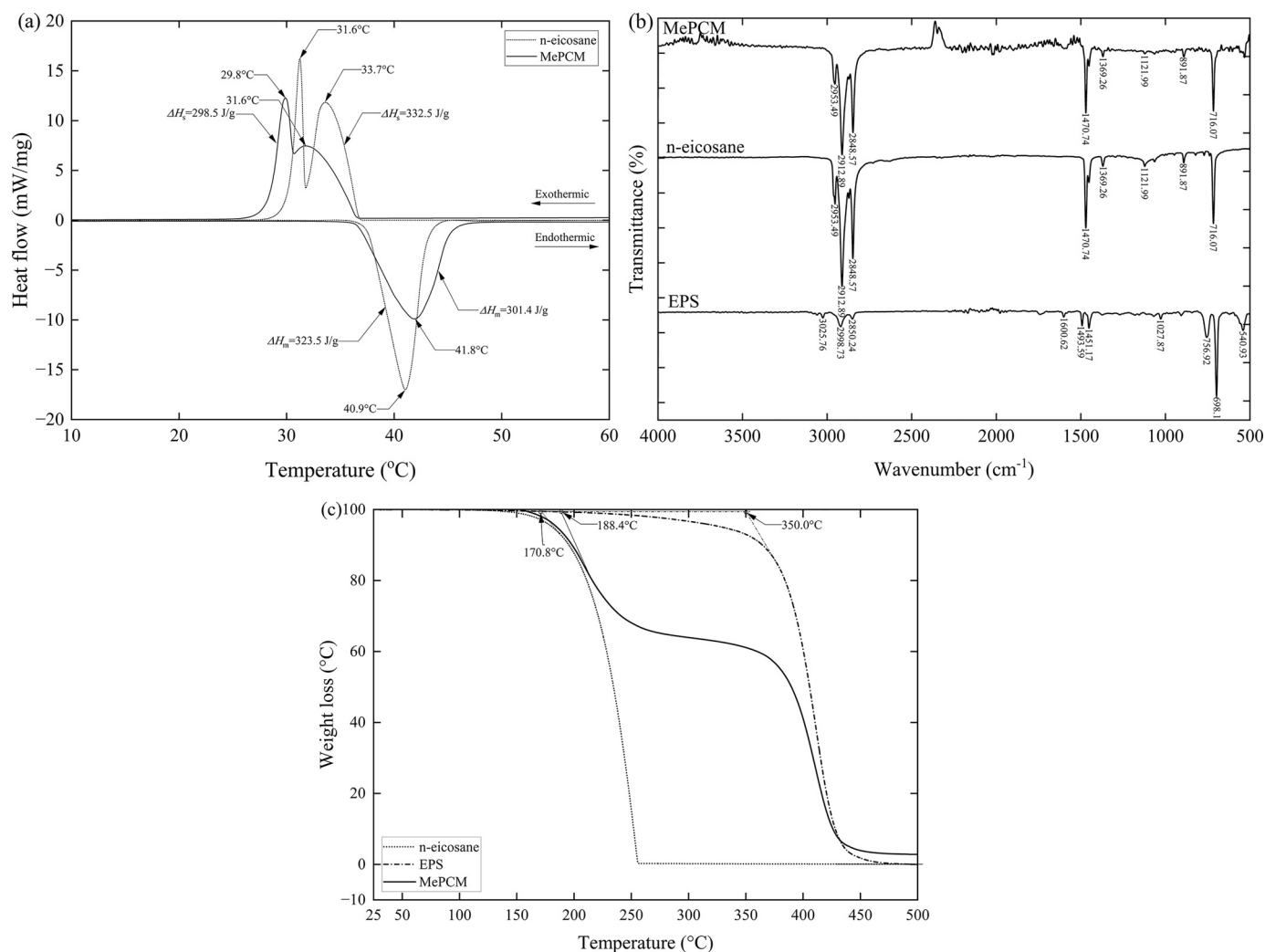


Fig. 3. Thermophysical characterization: (a) DSC thermograms; (b) FT-IR spectra; (c) TGA analysis.

Table 1
Thermal properties of n-eicosane and MePCM.

Material	Melting Enthalpy, ΔH_m (J/g)	Solidification enthalpy, ΔH_c (J/g)	Encapsulation ratio (R)	Encapsulation efficiency (E)
n-eicosane	323.5	323.5	–	–
MePCM	301.4	298.5	93.04 %	91.45 %

gregates, which is equivalent to the energy demands of pure n-eicosane [13]. Another contributing factor is the higher core/shell ratio, as there is a direct relationship between this ratio and the latent heat of MePCM is equivalent. Studies have shown that as the core/shell ratio increases, the latent heat almost equal, accompanied by an encapsulation efficiency of 91.45 % which is align with existing literature [12]. It is worth highlighting that the equivalency of the melting and solidification enthalpies of MePCMs have significant practical implications for thermal energy storage in construction applications. These properties can enable efficient energy absorption and release, ensuring reliable phase transitions, improved thermal stability, and simple integration into concrete, gypsum, and plaster. Additionally, melting enthalpy of MePCMs can effectively shift thermal loads by absorbing heat during peak demand, thereby maintaining comfortable indoor temperatures and reducing reliance on mechanical heating and cooling systems.

The chemical composition of the synthesized MePCM was analyzed using FT-IR spectroscopy (Bruker Tensor-27 model) with a KBr disc. The FT-IR spectra in Fig. 3b exhibit notable peaks at 2912.89cm^{-1} and 2848.57cm^{-1} , corresponding to asymmetric stretching and symmetric vibrations of C-H bonds in CH_3/CH_2 groups. A peak at 1470.74cm^{-1} indicates C = O bond stretching in the -COOH group, typical for organic PCMs. Distinct peaks at 1301cm^{-1} and 723cm^{-1} are associated with specific molecular vibrations; the 1369.26cm^{-1} peak represents C-H bending vibration, and 716.07cm^{-1} corresponds to CH_2 group's in-plane deformation rocking vibration. An additional peak at 891.87cm^{-1} , differing from the expected 940.12cm^{-1} , is attributed to -OH group vibrations. No new peaks are observed in the MePCM spectra, confirming their chemical stability, with an extra peak may be attributed to the shell material.

Thermogravimetric Analysis (TGA) was carried out using a TA SDT 650 instrument with a nitrogen flow rate of 100 mL/min. TGA analysis in Fig. 3c shows that the base PCM begins to lose weight at 170.8 °C, with no weight loss observed between 25 °C and 90 °C, defining this range as their operational temperature. Weight loss accelerates significantly after 170.8 °C and continues steadily until 256.8 °C, attributed to PCM evaporation. Note that beyond 200 °C, it loses 12.57 % by 256.8 °C. Similar observations are reported in [14]. In contrast, MePCMs exhibit enhanced thermal stability. No weight loss is detected until 150 °C, attributed to the thermal resilience of the PCM core and the protective shell. Degradation starts at 188.4 °C and undergoes a one-step decomposition between 188.4 °C and 349.2 °C as the shell material begins to

degrade. A second degradation step occurs up to 431.7 °C, with a total weight loss of 93.2 %. Unlike base PCMs, which degrade >99 % by this temperature, MePCMs demonstrate gradual decomposition up to 500 °C, achieving complete degradation only at this point.

4. Conclusions

This study synthesized MePCM from EPS nanoparticles derived from industrial waste using a surfactant-free Pickering emulsion for building applications hot climate. The EPS nanoparticles, produced through a nanoprecipitation technique with a 70 % sonicator amplitude setting, resulted in better-sized nanoparticles averaging ~150 nm in diameter. These nanoparticles formed MePCM shells with n-eicosane cores, featuring smooth inner and rough, undulating outer surfaces around 12 μm in diameter. MePCM's melting and solidification enthalpies were almost equivalent with n-eicosane's, at 301.4J/g and 298.5J/g, respectively, underscoring their potential for enhancing thermal management in buildings located in hot climates. Future studies will investigate the integration of MePCMs into building envelopes, emphasizing their thermal efficiency, mechanical properties, and environmental performance under practical conditions.

Data availability

Data will be made available on request.

Declaration of competing interest

The authors declare that they have no known competing financial interests or personal relationships that could have appeared to influence the work reported in this paper.

CRediT authorship contribution statement

Abdin Bedada Huluka: Writing – review & editing, Writing – original draft, Visualization, Methodology, Formal analysis, Data curation,

Conceptualization. **S. Muthulingam:** Writing – review & editing, Writing – original draft, Supervision, Resources, Methodology, Funding acquisition, Conceptualization. **S. Manigandan:** Writing – review & editing, Visualization, Resources, Methodology. **Chandra Shekhar:** Writing – review & editing, Visualization, Investigation, Formal analysis.

References

- [1] G. Alva, Y. Lin, L. Liu, G. Fang, Synthesis, characterization and applications of microencapsulated phase change materials in thermal energy storage: a review, *Energy Build.* 144 (2017) 276–294.
- [2] S. Drissi, T.-C. Ling, K.H. Mo, A. Eddahhak, A review of microencapsulated and composite phase change materials: alteration of strength and thermal properties of cement-based materials, *Renewable Sustainable Energy Rev.* 110 (2019) 467–484.
- [3] J. Giro-Paloma, M. Martínez, L.F. Cabeza, A.I. Fernández, Types, methods, techniques, and applications for microencapsulated phase change materials (MPCM): a review, *Renewable Sustainable Energy Rev.* 53 (2016) 1059–1075.
- [4] P.K. Singh Rathore, S.K. Shukla, N.K. Gupta, Potential of microencapsulated PCM for energy savings in buildings: a critical review, *Sustain Cities Soc.* 53 (2020) 101884.
- [5] K. Ghasemi, S. Tasnim, S. Mahmud, PCM, nano/microencapsulation and slurries: a review of fundamentals, categories, fabrication, numerical models and applications, *Sustainable Energy Technol. Assess.* 52 (2022) 102084.
- [6] A. Ismail, J. Wang, B. Abiodun Salami, L.O. Oyedele, G.K. Otukogbe, Microencapsulated phase change materials for enhanced thermal energy storage performance in construction materials: a critical review, *Constr. Build Mater.* 401 (2023).
- [7] M. Delgado, A. Lázaro, J. Mazo, B. Zalba, Review on phase change material emulsions and microencapsulated phase change material slurries: materials, heat transfer studies and applications, *Renewable Sustainable Energy Rev.* 16 (1) (2012) 253–273.
- [8] A. Rajeev, V. Erappalapati, N. Madhavan, M.G. Basavaraj, Conversion of expanded polystyrene waste to nanoparticles via nanoprecipitation, *J. Appl. Polym. Sci.* 133 (4) (2016).
- [9] R. Saxena, D. Rakshit, S.C. Kaushik, Experimental assessment of Phase Change Material (PCM) embedded bricks for passive conditioning in buildings, *Renew. Energy* 149 (2020) 587–599.
- [10] N. Shalkevich, A. Shalkevich, T. Bürgi, Thermal Conductivity of Concentrated Colloids in Different States, *J. Phys. Chem. C* 114 (21) (2010) 9568–9572.
- [11] S.K. Das, S.U. Choi, W. Yu, T. Pradeep, *Nanofluids: Science and Technology*, John Wiley & Sons, 2007.
- [12] J.Y. Do, N. Son, J. Shin, R.K. Chava, S.W. Joo, M. Kang, n-Eicosane-Fe₃O₄@SiO₂@Cu microcapsule phase change material and its improved thermal conductivity and heat transfer performance, *Mater. Design* 198 (2021) 109357.
- [13] C. Alkan, Enthalpy of melting and solidification of sulfonated paraffins as phase change materials for thermal energy storage, *Thermochim Acta* 451 (1) (2006) 126–130.
- [14] W. Su, J. Darkwa, T. Zhou, D. Du, G. Kokogiannakis, Y. Li, L. Wang, L. Gao, Development of Composite Microencapsulated Phase Change Materials for Multi-Temperature Thermal Energy Storage, *Crystals* 13 (8) (2023) 1167.